Weeks 9-10: Cosmic Microwave Background Fluctuations

April 12, 2017

We will follow Ch. 7 in Weinberg's book primarily, although the discussion here will be a combination of guide through Weinberg's calculation, rather than detailed re-derivation, and then a description of the resulting temperature power spectra. We again simplify as we did last week by ignoring the photon polarization, and we will consider only scalar perturbations (not tensor). The goal of this week will be to understand why the CMB temperature power spectrum looks like this:

1 The CMB fluctuation induced by a single Fourier mode

To begin, we return to the dimensionless intensity $J(\vec{x}, \hat{p}, t)$ and note that if evaluated today, at time t_0, and at our position, which we take to be $\vec{x} = 0$, then becomes $J(\vec{x} = 0, -\hat{n}, t_0)$ the CMB specific intensity we observe from a direction $\hat{n}$ on the sky. Moreover, since for a blackbody $J \propto T^4$, the fractional temperature perturbation we observe in direction $\hat{n}$ is $\Delta T(\hat{n})/T_0 = J(\vec{x} = 0, -\hat{n}, t_0)$. Recall further that we wrote the contribution to J of a Fourier mode of wavevector $\vec{q}$ as $J(\vec{q}, \hat{p}, t) = \alpha(\vec{q})\Delta_T(q, \mu = \hat{q} \cdot \hat{p}, t)$, with $\alpha(\vec{q})$ the primordial amplitude, set presumably by inflation, of the mode. Therefore, if we have a primordial density distribution specified by some set of $\alpha(\vec{q})$'s, the CMB temperature fluctuation we will see from position $\hat{n}$ is given by

$$\frac{\Delta T(\hat{n})}{T_0} = \frac{1}{4}\int d^3q\, \alpha(\vec{q})\Delta_T(q, -\hat{q} \cdot \hat{n}, t_0). \tag{1}$$

Recall now that for each value of $\vec{q}$, Δ_T satisfies a Boltzmann equation, an integro-differential equation for μ and t,

$$\dot{\Delta}_T(q,\mu,t) + i\frac{q\mu}{at(t)}\Delta_T(q,\mu,t) = -\omega_c(t)\Delta_T(q,\mu,t) - 2\dot{A}_q(t) + 2q^2\mu^2\dot{B}(t) + 3\omega_c(t)\Phi(q,t) + 4iq\mu\omega_c(t)\delta u_B(t). \tag{2}$$

The left-hand side accounts for the effects of expansion and free-streaming of the photon. The first term on the right describes the effects of scattering of photons from the direction $\hat{q}$. The second two describe the deflection of the photon trajectory in the metric perturbation. The Φ term accounts for the addition of photons with direction $\hat{q}$ from Thomson scattering from other directions. And the last term describes the Doppler shift in the intensity if the scatterers (here, electrons which during early times are tightly coupled to the photons) are moving.

As shown in Weinberg (and as you can easily verify), this equation (which is a linear first-order differential equation in time t) has a formal solution (valid well after recombination),

$$\begin{aligned}\Delta_T(q,\mu=\hat{q}\cdot\hat{n},t_0) &= \int_{t_1}^{t_0} dt\, \exp\left[i\mu q\int_t^{t_0}\frac{dt'}{a(t')}-\int_t^{t_0}dt'\,\omega_c(t')\right] \\ &\quad\times\left[-2\dot{A}(t)+2q^2\mu^2\dot{B}(t)+3\omega_c(t)\Phi(q,t)-4iq^2\mu^2\omega_c(t)\delta_B(t)/a(t)\right], \quad (3)\end{aligned}$$

where t_1 is some early initial time (taken to be well before recombination). With some algebraic re-arrangement, this can be separated into two parts, $\Delta_T = \Delta_T^{\rm early} + \Delta_T^{\rm isw}$, with

$$\begin{aligned}\Delta_T^{\rm early}(q,\mu,t_0) &= \int_{t_1}^{t_0} dt\, P(t), e^{iq\mu[\tau_0-\tau(t')]}\,[3\Phi(q,t) \\ &\quad -2a^2(t)\ddot{B}(t)-2a(t)\dot{a}(t)\dot{B}(t)-iq^2\mu^2\left(2\delta_B(t)/a(t)+2a(t)\dot{B}(t)\right)\Big], \quad (4)\end{aligned}$$

where $\tau(t)$ is the conformal time, and

$$\Delta_T^{\rm isw}(q,\mu,t_0) = -2\int_{t_1}^{t_0} dt\,\exp\left[iq\mu\,[\tau_0-\tau(t)]-\int_t^{t_0}dt'\,\omega_c(t')\right]\frac{d}{dt}\left[A(t)+a^2(t)\ddot{B}(t)+a(t)\dot{a}(t)\dot{B}(t)\right]. \quad (5)$$

Here, the function,

$$P(t) = \omega_c(t)\exp\left(-\int_t^{t_0} dt'\omega_c(t')\right), \quad (6)$$

is the visibility function, the probability that a given CMB photon last scatters at time t. It is defined so that

$$\int_{t_1}^{t_0} P(t)\,dt = 1. \quad (7)$$

Since $\omega_c(t)$ drops sharply near the redshift z_r of recombination from something huge compared with the expansion rate to something extremely small, $P(t)$ is narrowly centered around the time of recombination.

If we now make the approximation that recombination occurs suddenly at redshift z_c, at time t_c, then $P(t)$ is approximated as a delta function, and the time integral in Eq. (4) goes away. With this approximation, we can also assume tight coupling until recombination in which case $\Phi = \Delta_{T,0}/3 = 4\delta T/(3\bar{T})$. We then have

$$\Delta_T^{\rm early}(q,\mu,t_0) = e^{iq\mu[\tau_0-\tau_L]}\,[F(q)+i\mu G(q)], \quad (8)$$

with

$$\begin{aligned}F(q) &= 4\frac{\delta T(t_L)}{\bar{T}(t_L)}-\frac{1}{2}a^2()\ddot{B}(t_L)-\frac{1}{2}a(t_L)\dot{a}(t_L)\dot{B}(t_L), \quad (9)\\ G(q) &= -4q\left(\delta u_\gamma(t_L)/a(t_L)+a(t_L)\dot{B}(t_L)/2\right). \quad (10)\end{aligned}$$

Likewise, the ISW term becomes

$$\Delta_T^{\rm isw}(q,\mu,t_0) = -2\int_{t_1}^{t_0} dt\, \exp\left(iq\mu\left[\tau_0-\tau(t)\right]\right)\frac{d}{dt}\left[A(t)+a^2(t)\ddot{B}(t)+a(t)\dot{a}(t)\dot{B}(t)\right]. \qquad (11)$$

Let's now look at Eq. (8), which is not too complicated. It tells us that the CMB temperature fluctuation induced at the surface of last scatter by a Fourier mode $\vec{q}$. The $e^{iq\mu(ta u_0-\tau_L)}$ factor accounts for the sinusoidal variation associated with the particular Fourier mode. Associated with given Fourier mode is a real part and an imaginary part, out of phase, but only the real part is physical. The function $F(q)$ thus describes the amplitude of the sine, say, and $G(q)$ the amplitude of the cosine. The $F(q)$ factor accounts for some combination of the intrinsic radiation-temperature fluctuation and metric perturbation at the given point at the surface of last scatter. In Newtonian gauge, this factor becomes $F(q) = \Phi_q(t_L) + \delta T_q(t_L)/\bar{T}(t_L)$ which for adiabatic initial conditions becomes $F(q) = \Phi_q(t_L)/3$. Although we should be cautious about applying Newtonian reasoning to this relativistic situation, the form of $G(q)$ suggests that we can think of this term as a temperature fluctuation induced by the Doppler shift due to the peculiar velocity, induced by this density perturbation, along the line of sight. The factor of i multiplying $G(q)$ arises then because the peculiar velocity associated with this particular mode is out of phase with the density perturbation. Eq. (8) is obtained by assuming an infinitely thin surface of last scatter. Roughly speaking, the effects of the finite width of the surface of last scatter can be obtained by multiplying $\Delta_T^{\rm early}$ by $\exp\left[-\int_0^{t_L}\Gamma(t)\,dt\right]$ which, as we saw above, suppresses small-scale power by some $e^{-q^2/q_{\rm Silk}^2}$.

The second term, the "integrated-Sachs-Wolfe" term, provides another (generally smaller) contribution to the temperature fluctuation due to the travel of the photon through time-varying gravitational fields along the line of sight. In Newtonian gauge, the quantity in the brackets in Eq. (11) reduces to $2\dot{\Phi}$. It can be shown (e.g., from the Newtonian Poisson equation $\Phi_q \propto H^2a^2\delta\rho$ and $a(t) \propto t^{2/3}$ during MD) that there is no contribution to the ISW effect during matter domination. There is thus a small early-ISW contribution shortly after recombination due to the small residual contribution of the radiation density to the expansion rate. There is also a small late-ISW effect that arises during cosmological-constant domination at redshifts $z \lesssim 1$.

2 The CMB power spectrum

From the observed temperature pattern, Eq. (1), we can obtain the spherical-harmonic coefficients,

$$T_{\ell m} = \int d^2\hat{n} Y^*_{\ell m}(\hat{n})\frac{\Delta T(\hat{n})}{T_0}. \qquad (12)$$

This, along with the normalization $\langle\alpha(\vec{q})\alpha^*(\vec{q}')\rangle = \delta^3(\vec{q}-\vec{q}')$, and the plane-wave expansion,

$$e^{i\hat{q}\cdot\hat{n}\rho} = 4\pi\sum_{ellm} i^\ell j_\ell(\rho)Y_{\ell m}(\hat{n})Y^*_{\ell m}(\hat{q}), \qquad (13)$$

allow us to infer that the temperature power spectrum C_ℓ, defined by

$$\langle a_{\ell m}a_{\ell' m'}\rangle = C_\ell\delta_{\ell\ell'}\delta_{mm'}, \qquad (14)$$

is **(check normalization!)**

$$C_\ell = \pi^2 \int q^2\, dq, |\Delta_{T\ell}(q)|^2\,. \tag{15}$$

This can be evaluated by numerically solving the Boltzmann hierarchy derived earlier.

Alternatively, the predicted power spectrum can be evaluated using the approximate expressions for $\Delta_T(q,\mu,t_0)$ derived above. To simplify, we will ignore the ISW term. Doing so, the power spectrum can be approximated,

$$C_\ell = 16\pi^2 \int_0^\infty q^2\, dq\, \left|j_\ell(q\Delta\tau)F(q) + j'_\ell(q\Delta\tau)G(q)\right|^2 e^{-2q^2/q_{\rm Silk}^2}. \tag{16}$$

Note that the derivative on the spherical harmonic in the second term arises through an integration by parts. Here $\Delta\tau = \tau_0 - \tau_L$ is essentially the comoving distance to the surface of last scatter. For $\ell \gg 1$ the spherical Bessel function $j_\ell(x)$ is roughly zero for $x < \ell$ and then oscillates with a slowly decaying amplitude. From this, we infer that a given Fourier mode of wavenumber q contributes to fluctuation with $\ell \lesssim q\Delta\tau$, and the multipole moment ℓ receives contributions from wavenumbers $q \gtrsim \ell/\Delta\tau$ (**SIMPLE PICTURE**). But roughly speaking, each C_ℓ can be thought of, very roughly, as $C_\ell \sim 16\pi^2 q_\ell^3 \left[|F(q_\ell)|^2 + |G(q_\ell)|^2\right]$, with $q_\ell = \ell/\Delta\tau$.

The resulting power spectrum look like the following:

The features can be understood as follows: First, there is the Sachs-Wolfe plateau at $\ell \lesssim 100$. Recall that these angular scales probe modes that enter the horizon during matter domination. Since $G(q)$ probes peculiar velocities, this term should be negligible for these superhorizon modes, and we also inferred that $F(q) = \Phi/3$ in terms of the Newtonian potential, which is itself related to the primordial curvature perturbation by $\Phi = (3/5)\mathcal{R}$. In this case, the power spectrum becomes (for $\ell \ll 100$),

$$C_\ell^{\rm SW} \simeq \frac{2}{9\pi} \int q^2\, dq P_{\mathcal{R}}(q) \left[j_\ell(q\Delta\tau)\right]^2 P_{\mathcal{R}}(q). \tag{17}$$

Earlier, we derived a relation for $\Delta^2_{\mathcal{R}}(q) = [q^3/(2\pi^2)]P_{\mathcal{R}}(q) \propto V/\epsilon$, in terms of the inflaton-potential V and slow-roll parameter ϵ. Evaluating the integral, we then find, for a nearly scale-invariant spectrum, for $\ell \lesssim 100$,

$$\ell(\ell+1)C_\ell \propto \frac{V}{M_{\rm Pl}^4 \epsilon}. \tag{18}$$

From the measured value, $\ell(\ell+1)C_\ell \simeq 7 \times 10^{-10}$, we thus infer $\Delta^2_{\mathcal{R}} \simeq 2.2 \times 10^{-9}$ from which we infer an upper limit $V^{1/4} \lesssim 6.6 \times 10^{16}$ GeV, or if $\epsilon \lesssim 0.1$, $V^{1/4} \lesssim 3.6 \times 10^{16}$ GeV.

Acoustic peaks. Now let's consider the bumps and wiggles at $\ell \gtrsim 200$. These correspond to wavelengths that are at maximum compression (highest density) at the time of last scatter **(DRAW SZ PICTURE)**. The position of the first peak thus reflects the sound horizon at the surface of

last scatter, and the corresponding angle $\theta \simeq (\ell = 200)/\pi$ is that subtended by the sound horizon at the surface of last scatter. Note that the third peak is a bit higher than the second peak. This arises because the baryonic fluid is for the odd peaks moving in the same direction as the dark matter, while for even peaks it is moving in the opposite direction. There are then the troughs, which are nonzero. These are nonzero because in addition to the intrinsic radiation-temperature fluctuation, there is also a peculiar velocity associated with the density perturbation, and this is out of phase; when the radiation-density perturbation is zero, for a particular $\vec{q}$ mode, the peculiar velocity is maximal. This peculiar velocity induces a (smaller) Doppler shift in the temperature.

Silk dampling. There is then damping of the power at higher ℓ due to Silk damping which can also be understood as a blurring of the anisotropies on angular distances that probe physical distances smaller than the distance over which photons undergo their second-to-last scatter.

Late-time ISW effect Upon close inspection, you will see that there is a slight departure from flat $\ell(\ell+1)C_\ell$ at low ℓ. There are two reasons for this. First, the late-time ISW effect contributes at multipole moments $ell \lesssim 5$. This angular scale corresponds roughly to angle subtended by the horizon at redshift $z \simeq 1$ at which the cosmological constant becomes dynamically important.

Reionization. The second reason for an excess at $\ell \sim 10$ is reionization. Until now, we've supposed that electrons recombine at $z \simeq 1100$ and that photons streamed freely since then. However, at redshifts $z \lesssim 40$ gravitationally bound objects begin to form (as dicated by Press-Shechter theory). Objects with virial velocities large enough to allow hydrogen gas to cool and fragment into stars become abundant at redshifts $z \simeq 10-20$ (the details of these processes are highly uncertain). When the first stars form, they produce ultraviolet photons that reionize the Universe. If this occurs at $z \sim 10$, then roughly one in 10 CMB photons we see last scattered not near recombination, but at a redshift $z \sim 10$. This re-scattering does two things: First, it generates new fluctuations on angular scales $\ell \sim 10 - 20$ comparable to the angle subtended by the horizon at redshift $z \sim 10$ of reionization. These are generated essentially by re-scattering of photons from gas that—due to the existence of density perturbation—is moving toward or away from us. Second (and perhaps more important), if a fraction τ of photons re-scatter, then the power spectrum is suppressed by $e^{-2\tau}$ on multipoles $\ell \gtrsim 20$.

Early ISW effect. There is a contribution to C_ℓ at $\ell \lesssim 200$, in the rise to the first peak, from the early-ISW effect.

Spectral index. The cartoon shows the power spectrum for $n_s \simeq 1$. If n_s is larger (more power on small scales), the C_ℓ's get tilted toward higher ℓ and *vice versa* for lower ℓ.

The location of the first acoustic peak. The ℓ at which the first peak occurs is perhaps empirically the most precisely determined phenomenological parameter that describes the CMB. This quantity is determined by the angle subtended by the sound horizon at the surface of last scatter, and this angle is the comoving sound horizon at the surface of last scatter divided by the comoving distance to the surface of last scatter. This angle is increased (and ℓ thus decreased) if the sound horizon is larger, which can occur if the expansion rate prior to recombination is somehow decreased. The sound horizon is also decreased a bit if the baryon density is increased (although the Ω_b dependence is fairly weak). The comoving distance to the surface of last scatter is increased (and the value of $\ell_{\rm peak}$ increased) if the expansion rate is smaller in the post-recombination Universe, and *vice versa*

for larger expansion rate. Likewise, an increase in w, away from the cosmological-constant value $w > -1$, increases the expansion rate and thus decreases $\ell_{\rm peak}$, with all other parameters held fixed. There is a fairly strong dependence also on the spatial curvature. If the Universe is open, the peak moves to higher ℓ, and it moves to smaller ℓ in a closed Universe. The evidence from the CMB for a value of $\Omega_{\rm tot}$ that is very close to unity provides the most compelling evidence that our Universe is flat, or at least very close to flat.

3 Polarization for scalar perturbations

So far, we have assumed that photons are not polarized. The polarization changes the detailed quantitative results we have obtained so far (a result of the polarization dependence of Thomson scattering) but does not change the qualitative conclusions. The polarization is, however, observable, and the theory makes specific predictions for the power spectrum of the polarization as well as its cross-correlation with the temperature. There is also additional information, both in the way of additional statistical power and qualitatively different information, in the polarization.

We're not going to go through all the details in class—that would entail increasing significantly the complexity of the previously derived equations, without much additional insight. Instead, we will try to understand qualitatively what comes from the polarization.

Linear polarization arises through Thomson scattering. Light is fully linearly polarized when it scatters at a right angle. More generally, the differential cross section for Thomson scattering for a wave with initial polarization $\hat{\epsilon}$ to a final polarization $\hat{\epsilon}'$ is

$$\frac{d\sigma}{d\Omega} = \frac{3\sigma_T}{8\pi} \left| \hat{\epsilon} \cdot \hat{\epsilon}' \right|^2 . \tag{19}$$

Given that the cross section is thus proportional to a scattering $\cos^2\theta$, where θ is the scattering angle, it follows that if we have initially unpolarized radiation incident on a cloud of scatterers, the scattered radiation is polarized only if the incident radiation has an intensity quadrupole. In particular, if we have radiation incident on a cloud of scatterers, and the cloud has a Thomson-scattering optical depth τ, then the radiation scattered into the $\hat{z}$ direction will have polarization,

$$Q - iU = \sqrt{\frac{3}{40\pi}} \tau a_{22}, \tag{20}$$

where a_{22} is the coefficient of the spherical harmonic $Y_{22}(\theta, \phi)$ in a spherical-harmonic expansion of the incident-radiation intensity in a coordinate system in which the line of sight is in the $\hat{z}$ direction and the Stokes parameters Q and U are measured with respect to the x and y axes.

Well before recombination, when photons and baryons are tightly coupled, the radiation field at any given point has a negligible quadrupole moment—it is proportional to the inverse of the scattering rate. Near recombination, though, the photon mean-free path increases, the scattering rate decreases, and the quadrupole moment begins to grow. If we look at photons from a given point at the surface of last scatter, the radiation field incident on that last-scattering region most generally has a nonzero quadrupole, and so the radiation we see winds up having a polarization.

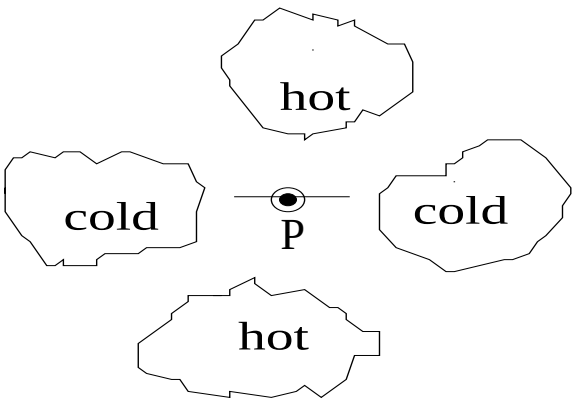

Figure 1: Light becomes fully polarized when it undergoes scattering by 90°. The polarization of light scattered in some region is thus proportional to the intensity (or temperature) quadrupole at that point.

The intensity quadrupole moment can be approximated by the tight-coupling approximation. Let's consider the photon Boltzmann equation we derived earlier.

$$\dot{\Delta}_{T,\ell}+\frac{q}{a(2\ell+1)}\left[(\ell+1)\Delta_{T,\ell+1}-\ell\Delta_{T,\ell-1}\right]=-2\dot{A}_q\delta_{\ell 0}+2q^2\left(\frac{\delta_{\ell 0}}{3}B_q-\frac{2\delta_{\ell 2}}{15}\right)-\omega_c\Delta_{T,\ell}+3\Phi\omega_c\delta_{\ell 0}-\frac{4}{3}q\omega_c\delta u_B\delta_{\ell 1}. \tag{21}$$

Let's consider the equation for $\ell=2$, the radiation quadrupole in the tight-coupling limit, $\omega_c \gg H$. In this case $\Delta_{T,3}$ is negligible by a factor $(\omega_c/H)^{-1}$. The terms proportional to A and B are negligible also compared with the other terms on the right-hand side. The terms on the left are the total time derivative for Θ_2, which we are trying to evaluate. We thus obtain,

$$\dot{\Delta}_{T2}=\frac{2}{5}\frac{q}{a}\Delta_{T1}+\omega_c\Delta_{T2}, \tag{22}$$

(the last term is actually multiplied by 9/10 when polarization dependence of photon scattering is taken into account). In the limit of large ω_c, the term on the left is negligible, and we find that

$$\Delta_{T2}\sim\frac{q}{a\omega_c}\Theta_{T1}. \tag{23}$$

From this, we infer that the phase of the polarization resembles that in the peculiar velocity. Recall, that the peaks in the temperature power spectrum are due to density perturbations, while the power in the troughs is contributed by the peculiar velocity (i.e., Δ_{T1}). It thus follows (and numerical results confirm) that the polarization power peaks are aligned in ℓ space with the troughs in the CMB power spectrum. The fact that $\Theta_{T2}\propto q\Delta_{T1}$ also implies that the polarization power spectrum $\ell^2C_\ell^{\rm EE}$ rises more rapidly as ℓ increases, and it then peaks at higher ℓ (more like $\ell\simeq 1000$ than does the temperature power spectrum, $\ell^2C_\ell^{\rm TT}$, which peaks at $\ell\simeq 200$.

Only E modes from density perturbations. We can also infer, without too much analysis, that density perturbations produce only E modes, and no B modes. To see this, consider a single Fourier mode of the density field in the $\hat{z}$ direction. The temperature pattern—and thus polarization pattern—produced by this mode must, by symmetry, be independent of ϕ, the azimuthal angle. The polarization must always be aligned or perpendicular to the lines of constant longitude. The variation of the polarization is thus always along directions parallel/perpendicular to the direction in which the polarization varies, and this is the hallmark of a pure E mode.

TE Cross correlation. Since some of the temperature fluctuation comes from the temperature dipole, which also sources the polarization, there is a temperature-polarization (TE) cross-correlation.

The reionization bump. As discussed above, the polarization power spectrum from the surface of last scatter becomes small as ℓ^2 as ℓ becomes small (large angular scales). But recall that a fraction $\tau\simeq 0.1$ of CMB photons re-scatter at a redshif $z\sim 10$. The reionized regions from which the photons re-scatter see a temperature quadrupole for the same reason that we do, and so the photons they re-scatter to us are polarized. The correlation scale of this reionization-induced polarization is the horizon at reionization, which subtends angles corresponding to $\ell\sim 10$. There is thus a large-angle reionization bump in the polarization power spectrum due to reionization. This polarization is correlated with the reionization-induced large-angle temperature bump, and so there is a large-angle bump also in the TE power spectrum. Since the polarization amplitude is so small, the signal is most easily seen in TE—i.e., through cross-correlation with the stronger temperature signal. This turns out to provide a unique constraint to the epoch of reionization. Measurement

of polarization on large angular scales is, however, notoriously difficult, and there is some tension between the $\tau \sim 0.9$-ish values WMAP obtained and the $\tau \sim 0.6$-ish values Planck is now getting. CLASS, a JHU-led project, should hopefully clarify the situation.

4 Tensor perturbations, polarization, and B modes

The Boltzmann-ology we worked out above for scalar metric perturbations can be altered to describe CMB fluctuations from primordial tensor metric perturbations (i.e., gravitational waves), such as those from inflation. The upshot is that inflationary tensor perturbations wind up producing a B mode in CMB polarization at $\ell \lesssim 100$. If slow-roll inflation describes how things transpired in the early Universe, then measurements that suggest $\epsilon \sim 0.1$ also suggest that this B-mode signal should be not too small. There is thus considerable effort focussed now on detecting these B modes.

Although there are some complications (e.g., the tensor structure and two polarizations of the tensor spacetime perturbation), calculation of CMB fluctuations for tensor perturbations entails a number of simplifications. First of all, there is no gauge degree of freedom to worry about. Second, the equation of motion for the spacetime metric is trivial—it is just a wave equation in an expanding Universe. Third, the signal becomes negligible at $\ell \gtrsim 100$ and so numerical evaluations are far simpler.

The discussion here is cut and paste from arXiv:1510.06042 by Ely Kovetz and me. We now show how gravitational waves induce temperature fluctuations and polarization in the cosmic microwave background. We first derive the angular distribution of photon intensities in the presence of a gravitational wave (GW). Suppose that the Universe is filled with photons that do not scatter. In this case, the photon energies are affected only by the form of the metric. Consider a single monochromatic plane-wave gravitational wave, which appears as a tensor perturbation to the FRW metric,

$$ds^2 = a^2(\tau)\left[d\tau^2 - dx^2(1+h_+) + dy^2(1-h_+) + dz^2\right], \tag{24}$$

where τ is the conformal time and

$$h_+(\vec{x},\tau) \simeq h(\tau)e^{ik\tau}e^{-ikz}, \tag{25}$$

describes a plane wave propagating in the $\hat{z}$ direction. This is a linearly-polarized gravitational wave with "+" (rather than "×") polarization. Here $h(\tau)$ is the amplitude; at early times when $k\tau \lesssim 1$, $h(\tau) \simeq$ const, but then $h(\tau)$ redshifts away when $k\tau \gtrsim 1$. If we construct the Einstein tensor $G_{\mu\nu}$ from the metric, Eq. (24), then the vacuum Einstein equation $G_{\mu\nu} = 0$ leads to the wave equation for $h_+(\vec{x},t)$. The "$\simeq$" sign appears in Eq. (25) because the gravitational waves do not propagate in a vacuum but rather in a Universe filled with a cosmic fluid. The anisotropic stress of this fluid (to which the neutrino background contributes after neutrinos decouple) modifies slightly the time evolution, a calculable $\sim 10\%$ correction to Eq. (25).

Photons that propagate freely through this spacetime experience a frequency shift $d\nu$ during an expansion interval $d\tau$ determined by the geodesic equation, which in this spacetime takes the form,

$$\frac{1}{\nu}\frac{d\nu}{d\tau} = -\frac{1}{2}(1-\mu^2)\cos 2\phi e^{-ikz}\frac{d}{d\tau}(he^{ik\tau}), \tag{26}$$

where μ is the cosine of the angle that the photon trajectory makes with the z axis, and ϕ is the azimuthal angle of the photon's trajectory. This redshifting is polarization-independent, but polarization is then induced by Thomson scattering of this anisotropic radiation field. To account for the polarization, we must follow the time evolution of four distribution functions (DFs) $f_s(\vec{x},\vec{q};\tau)$ where $\vec{q}$ is the photon momentum, for $s = I$, Q, U, and V, the four Stokes parameters required to specify the polarization. The original (unperturbed) distribution function is $\bar{f}_I(\vec{q},\vec{x};\tau) = \left[e^{h\nu/k_BT(\tau)} - 1\right]^{-1}$, where k_B is the Boltzmann constant and $T(\tau)$ the unperturbed CMB temperature at conformal time τ, and $\bar{f}_Q = \bar{f}_U = \bar{f}_V = 0$. We then define perturbations $\Delta_s e^{i\vec{k}\cdot\vec{x}} = 4\delta f_s/(\partial\bar{f}/\partial\ln T)$, suppressing an index $\vec{k}$ for notational economy. Thomson scattering induces no ciruclar polarization, so $\Delta_V = 0$ at all times. Since the gravitational redshift and Thomson scattering are frequency independent, the evolution of the distribution function is the same for all frequencies. Since the $e^{i\vec{k}\cdot\vec{x}}$ spatial dependence of the DFs is separated out in the definition of Δ_s, the perturbed DFs are functions $\Delta_s(\hat{q};\tau)$ only of the direction $\hat{q}$ of the photon and the conformal time τ. Finally, if we define perturbation variables $\tilde{\Delta}_s$ by

$$\Delta_I = \tilde{\Delta}_I(1-\mu)^2\cos 2\phi, \qquad \Delta_Q = \tilde{\Delta}_Q(1+\mu)^2\cos 2\phi, \qquad \Delta_U = \tilde{\Delta}_U 2\mu\sin 2\phi, \tag{27}$$

the new variables $\tilde{\Delta}_s(\mu;\tau)$ are now functions only of μ and there is a relation $\tilde{\Delta}_Q = -\tilde{\Delta}_U$ for the gravitational wave, a consequence of the fact that the orientation of the photon polarization is fixed by the direction of the photon with respect to the GW polarization tensor. As a result, the Boltzmann equations for the distribution functions reduce to two equations,

$$\dot{\tilde{\Delta}}_I + ik\mu\tilde{\Delta}_I = -\dot{h} - a\omega_c\left[\tilde{\Delta}_I - \Psi\right], \qquad \dot{\tilde{\Delta}}_Q + ik\mu\tilde{\Delta}_Q = -a\omega_c\left[\Delta_P + \Psi\right], \tag{28}$$

where here the dot denotes derivative with respect to conformal time. Here, the variable

$$\Psi \equiv \left[\frac{1}{10}\tilde{\Delta}_{I0} + \frac{1}{7}\tilde{\Delta}_{I2} + \frac{3}{70}\tilde{\Delta}_{I4} - \frac{3}{5}\tilde{\Delta}_{Q0} + \frac{6}{7}\tilde{\Delta}_{Q2} - \frac{3}{70}\tilde{\Delta}_{Q4}\right], \tag{29}$$

is given in terms of the Legendre moments $\tilde{\Delta}_{I\ell}(\tau) = (1/2)\int_{-1}^{1} d\mu\,\tilde{\Delta}_I(\mu;\tau)P_\ell(\mu)$ (and similarly for $\tilde{\Delta}_{Q\ell}$), where $P_\ell(\mu)$ is a Legendre polynomial. The quantity ω_c is, as before, the scattering rate.

Eqs. (28) and (29) look complicated but describe relatively simple physics. The left-hand sides of Eq. (28) are simply the Lagrangian time derivatives for a Fourier mode of wavenumber k. The $\dot{h}$ in the first equation accounts for the intensity variation (described above) induced by the gravitational redshift; its absence from the second equation is because the gravitational redshift is polarization-independent. As the presence of the scattering rate ω_c suggests, the terms on the right-hand sides of Eqs. (28) involving Ψ, $\tilde{\Delta}_I$, and $\tilde{\Delta}_P$ account for Thomson scattering. They are derived using the dependence $d\sigma_T/d\Omega \propto (\hat{\epsilon}_i\cdot\hat{\epsilon}_f)^2$ of the Thomson differential cross section on the polarization vectors $\hat{\epsilon}_i$ and $\hat{\epsilon}_f$ of the initial- and final-state photons. This dependence also explains why a quadrupolar anisotropy in the incoming radiation is required in order to generate the linear polarization signal.

Still, Eqs. (28) and (29) constitute a set of coupled partial integro-differential equations. In practice, they are solved numerically by expanding $\tilde{\Delta}_I$ and $\tilde{\Delta}_Q$ in terms of their Legendre moments and thus recasting the equations as an infinite set of coupled Boltzmann equations for $\tilde{\Delta}_{I\ell}(\tau)$ and $\tilde{\Delta}_{Q\ell}(\tau)$. They are then solved numerically by integrating from some early time and truncating the hierarchy at some sufficiently high ℓ.

Later we will return to these equations, but for now we show in Fig. 2(b) the resulting CMB temperature-polarization pattern induced by one gravitational wave propagating in the $\hat{z}$ direction.

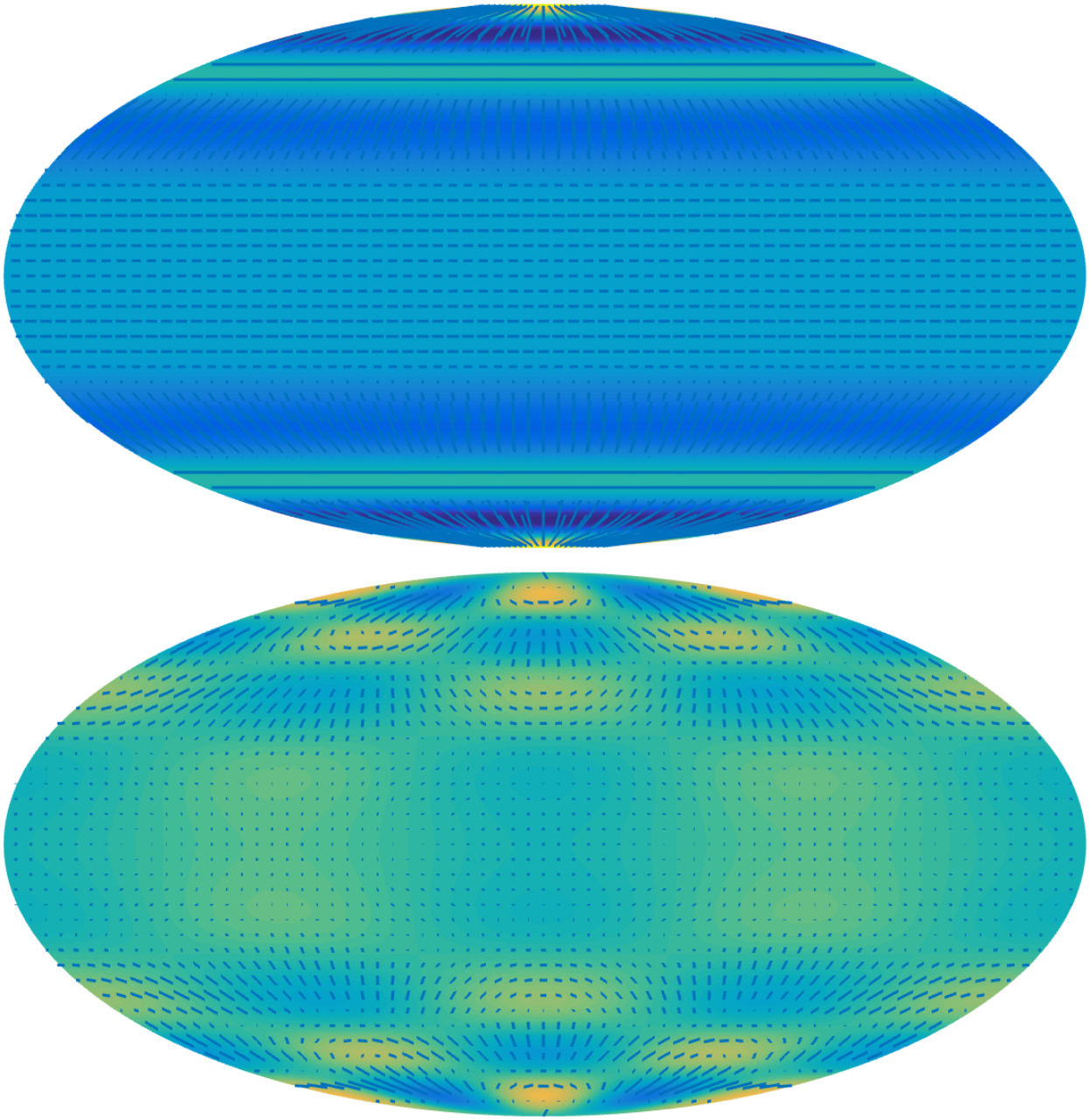

Figure 2: (a) The CMB temperature-polarization pattern induced by one Fourier mode of the density field (i.e., a scalar metric perturbation). The polarization pattern varies along a direction parallel/perpendicular to lines of constant longitude that align with the direction of the wave. The induced polarization pattern is thus a pure E mode. (b) The same for a single gravitational wave (i.e., a single Fourier mode of the tensor field). We see that in this case, there is variation of the polarization not only parallel/perpendicular to lines of constant longitude, but also along directions 45° with respect to these lines. There is thus a B mode induced.

The quadrupolar variation (i.e., the $\cos 2\phi$ dependence) of the temperature-polarization pattern can be seen as one travels along a curve of constant latitude, and the wavelike pattern can be seen as one moves along a line of constant longitude. It can be seen that as we move along the line of constant longitude, there are variations in Q, the component of the polarization perpendicular/parallel to those constant-longitude lines. It can also be seen, however, that there are variations in U, the component of the polarization 45° with respect to constant-longitude lines. This, as we will see below, is a signature of the B mode in the CMB polarization pattern induced by the gravitational wave. This is to be contrasted with the polarization pattern, shown in Fig. 2(a), for a single Fourier mode of the density field. In this case, there is no variation along lines of constant latitude, and there is only variation in Q, and thus no B mode.

5 E and B modes from gravitational waves

The upshot of the above discussion is that the gravitational wave in the $\hat{z}$ direction, with + polarizatoin, induces a polarization tensor,

$$\mathcal{P}^{ab}_{\vec{k},+}(\theta,\phi) = \frac{T_0}{4\sqrt{2}}\sum_\ell (2\ell+1)P_\ell(\cos\theta)\tilde{\Delta}_{Q\ell}\begin{pmatrix} (1+\cos^2\theta)\cos 2\phi & 2\cot\theta\sin 2\phi \\ 2\cot\theta\sin 2\phi & -(1+\cos^2\theta)\csc^2\theta\cos 2\phi \end{pmatrix}. \tag{30}$$

If we expand this in tensor spherical harmonics, the resulting coefficients are

$$a^{\mathrm{E}\,\tilde{\mathrm{k}},+}_{\ell m} = \frac{\sqrt{\pi(2\ell+1)}}{4(\delta_{m,2}+\delta_{m,-2})^{-1}}\left[\frac{(\ell+2)(\ell+1)\tilde{\Delta}_{Q,\ell-2}}{(2\ell-1)(2\ell+1)} + \frac{6\ell(\ell+1)\tilde{\Delta}_{Q\ell}}{(2\ell+3)(2\ell-1)} + \frac{\ell(\ell-1)\tilde{\Delta}_{Q,\ell+2}}{(2\ell+3)(2\ell+1)}\right], \tag{31}$$

and

$$a^{\mathrm{B}\,\tilde{\mathrm{k}},+}_{\ell m} = \frac{-i}{2\sqrt{2}}\sqrt{\frac{2\pi}{(2\ell+1)}}(\delta_{m,2}-\delta_{m,-2})\left[(\ell+2)\tilde{\Delta}_{Q,\ell-1} + (\ell-1)\tilde{\Delta}_{Q,\ell+1}\right]. \tag{32}$$

We have thus shown explicitly that both the E and B components are nonzero for a gravitational wave, confirming the heuristic arguments above.

This particular gravitational wave (in the $\hat{z}$ direction with + polarization) contributes

$$C_\ell^{\mathrm{BB},\vec{k},+} = \frac{1}{2l+1}\sum_m |a^B_{\ell m}|^2 = \frac{\pi}{2}\left[\frac{\ell+2}{2\ell+1}\tilde{\Delta}_{Q,\ell-1} + \frac{\ell-1}{2\ell+1}\tilde{\Delta}_{Q,\ell+1}\right]^2. \tag{33}$$

to the BB power spectrum, and similarly for C_ℓ^{EE}, with the replacement B→E in Eq. (33). Since C_ℓ^{BB} is a rotationally invariant quantity, any gravitational wave of this wavenumber k pointing in any direction, with either polarization, will contribute similarly to C_ℓ^{BB}. We thus obtain the BB power spectrum from the stochastic gravitational-wave background by summing all Fourier modes, $\int d^3k/(2\pi)^3$, and over both gravitational-wave polarization states. The final result for C_ℓ^{BB} is thus,

$$C_\ell^{\mathrm{BB}} = \frac{1}{2\pi}\int k^2\,dk\left[\frac{\ell+2}{2\ell+1}\tilde{\Delta}_{Q,\ell-1}(k) + \frac{\ell-1}{2\ell+1}\tilde{\Delta}_{Q,\ell-1}(k)\right]^2, \tag{34}$$

and analogously for C_ℓ^{EE}. Note that the cross-correlation power spectrum vanishes, $C_\ell^{\mathrm{EB}} = \sum_{m=-\ell}^{m=\ell}(a^{\mathrm{E}*}_{\ell m}a^{\mathrm{B}}_{\ell m})/(2\ell+1) = 0$, as it should, because $a^{\mathrm{E}}_{(\ell m)} \propto (\delta_{m,2}+\delta_{m,-2})$, while $a^{\mathrm{B}}_{(\ell m)} \propto (\delta_{m,2}-\delta_{m,-2})$ for a + polarization gravitational wave propagating in the $\hat{z}$ direction, and similarly for C_ℓ^{TB}.

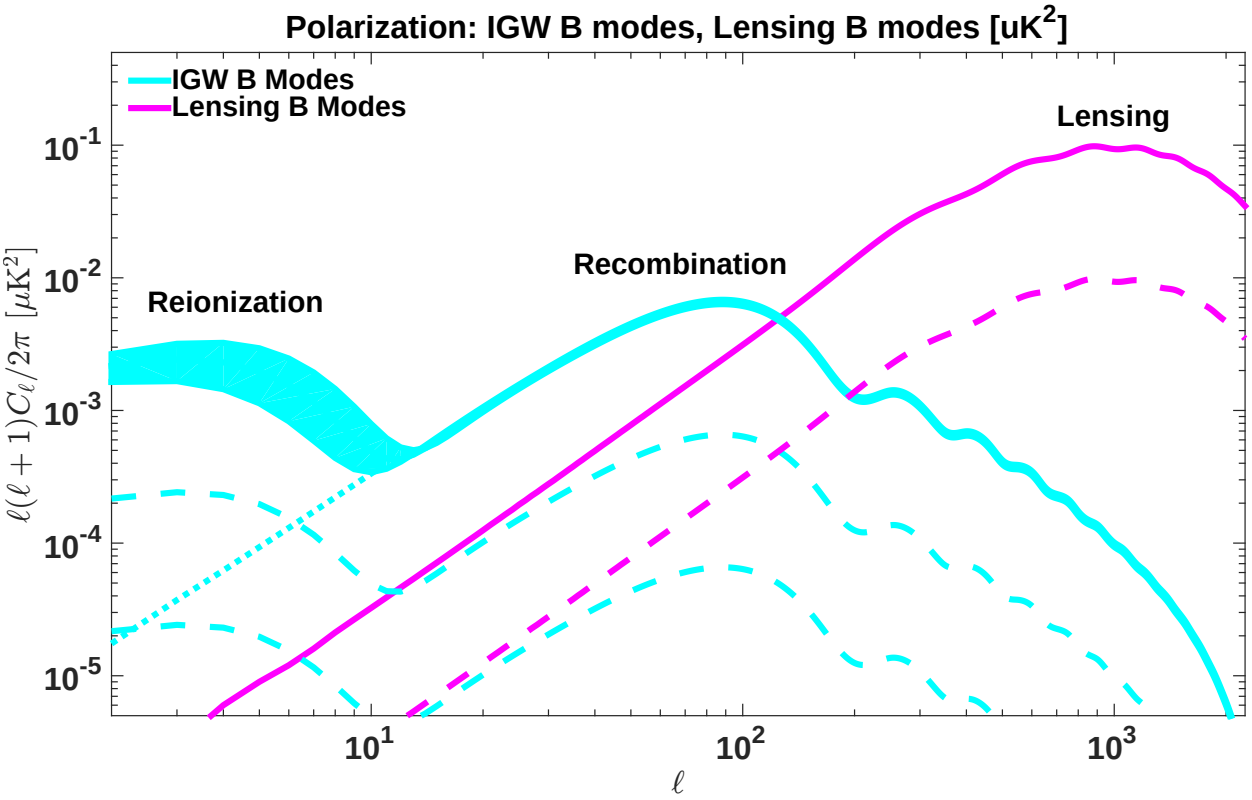

Figure 3: *Polarization power*: Spectra are shown for primordial B modes with $r = \{0.1, 0.01, 0.001\}$ (*cyan*), lensing-induced B modes (*magenta*), as well as scalar E modes (*red*), for comparison. The $\pm 1\sigma$ uncertainty due to the current τ constraint is indicated for the $r = 0.1$ case by the (*cyan*) shading. A 90% delensed signal is also shown for comparison (*dashed-magenta*). Plots were generated using CAMB with Planck 2015 best-fit parameters.

Fig. 3 shows results of numerical evaluation of Eq. (34) using CAMB, with the Planck 2015 cosmological parameters. The "recombination peak" in the power spectrum [multiplied by $\ell(\ell+1)/2\pi$] at $\ell \sim 100$ arises from gravitational waves that enter the horizon around the time of CMB decoupling at redshift $z \simeq 1100$. The power drops at smaller ℓ because longer-wavelength modes were superhorizon at the time of decoupling and thus have a suppressed effect on subhorizon physics. The power drops at higher ℓ because the amplitudes of shorter-wavelength gravitational waves, which entered the horizon earlier, have begun redshifting away by the time of CMB decoupling. The "reionization bump" at $\ell \lesssim 10$ arises from re-scattering of the CMB by free electrons that were reionized at redshift $z \sim 8$ by ultraviolet radiation from the first stars. The wiggles at higher ℓ arise from the difference in phases of gravitational waves at different wavelengths at the time of CMB decoupling. The overall amplitude scales with the tensor-to-scalar ratio r.